ELSEVIER

Palaeogeography, Palaeoclimatology, Palaeoecology 111 (1994) 83–98

PALAEO

New AMS dates, stratigraphic correlations and decadal climatic cycles for the past 4 ka at Lake Turkana, Kenya

John D. Halfman [a], Thomas C. Johnson [b,1], Bruce P. Finney [c]

[a] *Department of Civil Engineering and Geological Sciences, University of Notre Dame, Notre Dame, Indiana 46556-0767, USA*

[b] *Department of Geology, Duke University Marine Laboratory, Beaufort, NC 28516, USA*

[c] *Institute of Marine Science, School of Fisheries and Ocean Sciences, University of Alaska, Fairbanks, Fairbanks, Alask 99775, USA*

Received 20 July 1993; revised and accepted 10 January 1994

Abstract

New AMS radiocarbon dates and stratigraphic correlations of 7 piston cores recovered from Lake Turkana, Ea Africa, show that the frequency of cyclic variability is greater than previously reported for a single piston core. Almo 60 new AMS dates of various carbonate fractions indicate that large (>150 μm) ostracode carapaces yield the mo accurate chronology for the sediment record due to the input of "old" fine-grained carbonate. Stratigraphic correlatio among the cores by carbonate abundance and magnetic susceptibility profiles provide supporting evidence for tl ostracode-based chronology. This chronology refines earlier estimates of sediment accumulation that impacts tl recurrence interval of lamination deposition from one lamination every two years to one lamination per year in tw north basin cores. The record of carbonate content within the north basin of the lake reflect its dilution wi terrigenous sediments input from the Omo River but direct paleoclimatic interpretations are complicated by later migrations of the delta channels with changing lake levels. Time-series analysis of both individual cores and combined carbonate profile show significant spectral peaks at >1000, 76, 32, 22, 18.6 and 11 yr. The latter thr suggest an important link between the sediments accumulating in Lake Turkana and global cycles of climat variability.

1. Introduction

Decade-to-century scale, cyclic variability was reported from a single piston core, LT84-8P, recovered from the north basin of Lake Turkana, Kenya. Down-core profiles of bulk carbonate content, lamination thickness (Halfman and Johnson, 1988) and stable isotope ratios of fine-grained carbonate (Johnson et al., 1991) revealed consistent periods on a century time scale; the lamination data suggested additional periods on decade time scale. The authors proposed that thi core was representative of sedimentation durin the late Holocene for the entire basin, and tha both carbonate content and lamination thicknes were dependant on discharge of the Omo Rive oxygen isotopic composition of the carbonates wa dependant on water chemistry, and five conven tional radiocarbon dates accurately described sedi ment accumulation at the site. The goal of thi paper is to increase the chronologic control of an to determine if higher-frequency cycles exists i the carbonate record by analyzing approximatel

[1]Present address: Large Lakes Observatory, University of Minnesota, Duluth, MN 55812, USA.

SSDI 0031-0182(94)00007-U

60 accelerator radiocarbon dates, increasing the carbonate sample resolution, and providing independent chronologic tests with stratigraphic correlations between this and other cores recovered from Lake Turkana.

2. Lake Turkana

Lake Turkana is the largest, closed-basin lake in the East African Rift System (Fig. 1). A shallow, basement controlled, bathymetric sill, adjacent to the Turkwel and Kerio Deltas, divides the lake into two basins. The lake occupies a hot and arid setting with mean annual temperatures of 30°C and annual rainfall less than 200 mm (Ferguson and Harbott, 1982). Discharge from the Omo River provides approximately 90% of the freshwater to the lake from its headwaters on the Ethiopian Plateau. The remaining fluvial input is primarily from the Turkwel and Kerio Rivers. The lake is moderately saline (2.5‰), alkaline (20 meq/l, pH 9.2) and well mixed by strong diurnal winds (Ferguson and Harbott, 1982; Yuretich and Cerling, 1983).

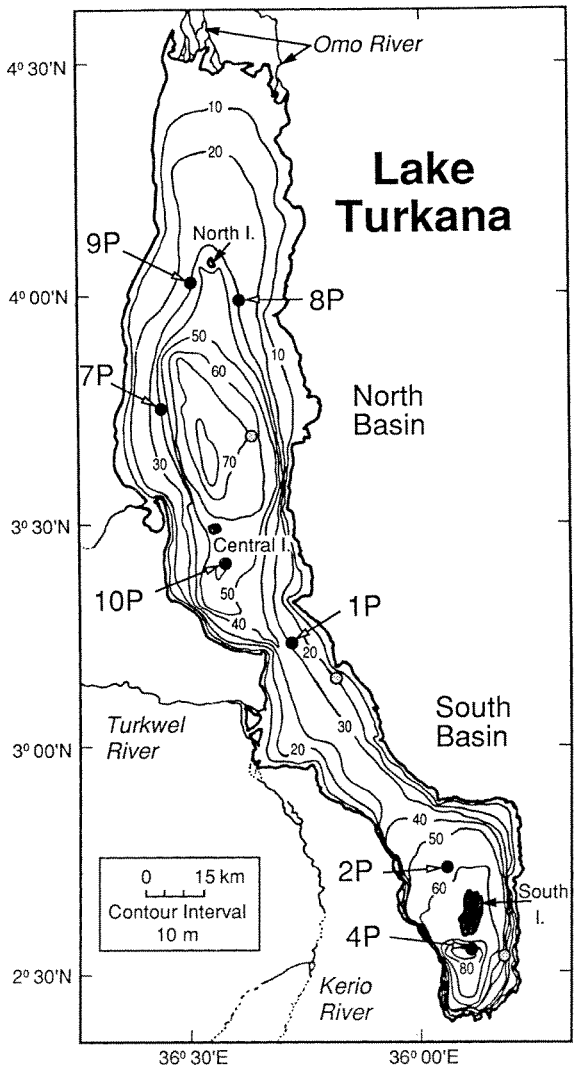

Fig. 1. Bathymetric map and core locations, Lake Turkana, Kenya.

The lake responds drastically to climate change. A compilation of historical data from the late 1800's to the mid 1970's reveals fluctuations in lake level over a 20 m range (Butzer, 1971). Since the early 1980's, lake level has continued to drop by a few meters (Halfman, unpublished data). Lake level has varied considerably during the past 12 ka from nearly desiccated conditions at the end of the Pleistocene to overflowing conditions during the early Holocene (Owen et al., 1982; Johnson et al., 1987). Changes in diatom assemblages from a south basin core are interpreted to reflect generally declining lake levels from the early Holocene pluvial to present day levels with a rapid change in lake level at about 4 ka (Halfman et al., 1992). The long-term trend is roughly synchronous with other basins throughout much of east Africa and is attributed to Milankovitch induced changes in the intensity of the northern tropical monsoon (Street-Perrott and Harrison, 1983; Kutzbach and Street-Perrott, 1985).

The modern profundal sediments are dominated by sandy to silty clays with a mineralogic and chemical composition that reflects the relative importance of Omo River input to the north, Turkwel-Kerio input to the central portion of the lake, and local sources along the eastern margin of the lake (Yuretich, 1976, 1986). Sedimentation rates are unusually high in Lake Turkana compared to other large lakes, on the order of 1–10 mm/yr in the upper 12 m of the sediment column (Halfman and Johnson, 1988; Halfman and Hearty, 1990; Halfman et al., 1992; this paper). Carbonate contents range from 1 to 25% (wt.%

$CaCO_3$) of the dry sediment (Yuretich, 1986; Halfman and Johnson, 1988). Most of it is authigenic, low-magnesium calcite; typically less than 20 μm in length (Halfman et al., 1989). The crystals are primarily euhedral, arrow-shaped blades. Stable isotope values suggest that the fine-grained calcite precipitates in surface-waters, not during early sediment diagenesis (Halfman et al., 1989; Johnson et al., 1991). Ostracode carapaces, and rare gastropod shells and beach rock fragments also contribute to the carbonate fraction of the profundal sediments (Cohen, 1984). Detrital carbonates were not detected in material discharged by the Omo River (Cerling et al., 1988).

3. Methods

Ten piston-cores, each approximately 12-m long by 6 cm in diameter, were collected in 1984 (Fig. 1). Forty-seven AMS radiocarbon dates were acquired from 6 cores (1P, 2P, 4P, 7P, 8P and 9P) to complement twelve AMS and nine conventional radiocarbon dates reported in Halfman and Johnson (1988), Halfman and Hearty (1990) and Halfman et al. (1992). Various carbonate fractions of the sediment were selected for dating because: (1) the organic carbon content of the sediments is very low (<1.5 wt%, Halfman, 1987); (2) the lake's high alkalinity and well mixed nature promotes rapid equilibration of carbon dioxide between the atmosphere and the lake; and, (3) SEM photography, and trace, pore water and stable isotope geochemistry suggest that only authigenic calcite and ostracodes carapaces are the abundant carbonate phases in the profundal sediments, and both are expected to precipitate in near-equilibrium with the water column.

Sediment samples were wet sieved at 63 and 150 μm to isolate the various carbonate fractions for AMS dating. The authigenic carbonate dominates all of the carbonate in sediment finer than 63 μm. Approximately 25–50 ostracode carapaces were picked from 63 to 150 μm or >150 μm fractions of sediment. Freeze-drying assisted in separating mud from the ostracode carapaces before washing with deionized water. Core intervals for each sample were typically 3–4 cm thick but were occasionally larger to ensure sufficient numbers of ostracodes from the north bas cores. Most of the reported dates were adjust for total isotope effects based on $\delta^{13}C$ measur ments, and are reported as radiocarbon years B. using a half-life of 5568 yr. The Stuiver and Reim (1993) calibration was used when radiocarbon ar calendar age conversions were required to compa paleoclimatic proxies. A few published dates we not analyzed for $\delta^{13}C$ but the ages were adjust assuming a $\delta^{13}C$ value of zero. The range reported $\delta^{13}C$ measurements is small (−4.4–0.1‰ PDB), so that the corresponding variability in a due to an incorrect $\delta^{13}C$ value is less than approx mately 100 years. The quoted errors represent or standard deviation of the detection statistics.

Carbonate abundance was determined for strat graphic correlations and cyclic variability on 1-cn sub-samples from cores 1P, 2P, 7P, 8P, 9P an 10P using a vacuum-gasometric technique (Jon and Kaiteris, 1983). Values are reported as weigh percent $CaCO_3$ of the dry sedimen Reproducibility of selected duplicate measur ments was ±0.25 wt%. Sample intervals wer increased from an average 35-cm interval used b Halfman and Johnson (1988) to about 3 cm dow cores 2P, 7P, 8P and 9P, and 10 cm down 1P an 10P in this study. These data were augmented wit 139 analyses for %Ca by flame atomic absorptio spectrometry on dilute acetic acid leaches of bul sediment to exclude non-carbonates. The %C values were converted to $\%CaCO_3$ using a linea regression through 27 samples with both %C (flame AA) and $\%CaCO_3$ (vacuum-gasometric determinations ($r^2=0.91$).

Magnetic susceptibility, κ, was measured fo additional stratigraphic correlations on archive sections of cores 1P, 2P, 4P, 7P, 8P, 9P and 10 using a Bartington Instruments MS 1 meter witl a low-field, 7-cm diameter, 2-cm wide loop. Value are reported as volume susceptibility. Sample spac ing was 1.5 cm down cores 7P, 8P and 9P, an 5 cm down 1P, 2P, 4P, and 10P. Desiccated sec tions of 10P at 0–30, 260–300, 445–480 an 730–755 cm were excluded. This data augment lower resolution data from cores 7P and 8 (Halfman and Hearty, 1990). Duplicate measure ments were within 1% of the respective mean o each depth.

Spectral analysis was performed on various carbonate data sets with the ARAND software package, which was provided by investigators at Oregon State University. The calculations are based on the Blackman-Tukey technique of the auto-correlation function after removing the long-term linear trend.

4. Geochronology

Radiocarbon dates on different carbonate fractions often exhibit significant variations, even from the same sediment sample. This is especially evident in core 8P where discrepancies of more than 2000 yr occur at several depths (Fig. 2). In this core, ostracodes coarser than 150 μm consistently date younger than either the fine-grained carbonate (micrite) or ostracodes finer than 150 μm. Similarly, micrite samples from four separate depths in core 2P are consistently older by an average of 350 years than corresponding ostracode samples isolated from the identical depths (Halfman et al., 1992). One explanation could be that bioturbation selectively mixes the fine carbonate fraction upwards into younger sediments.

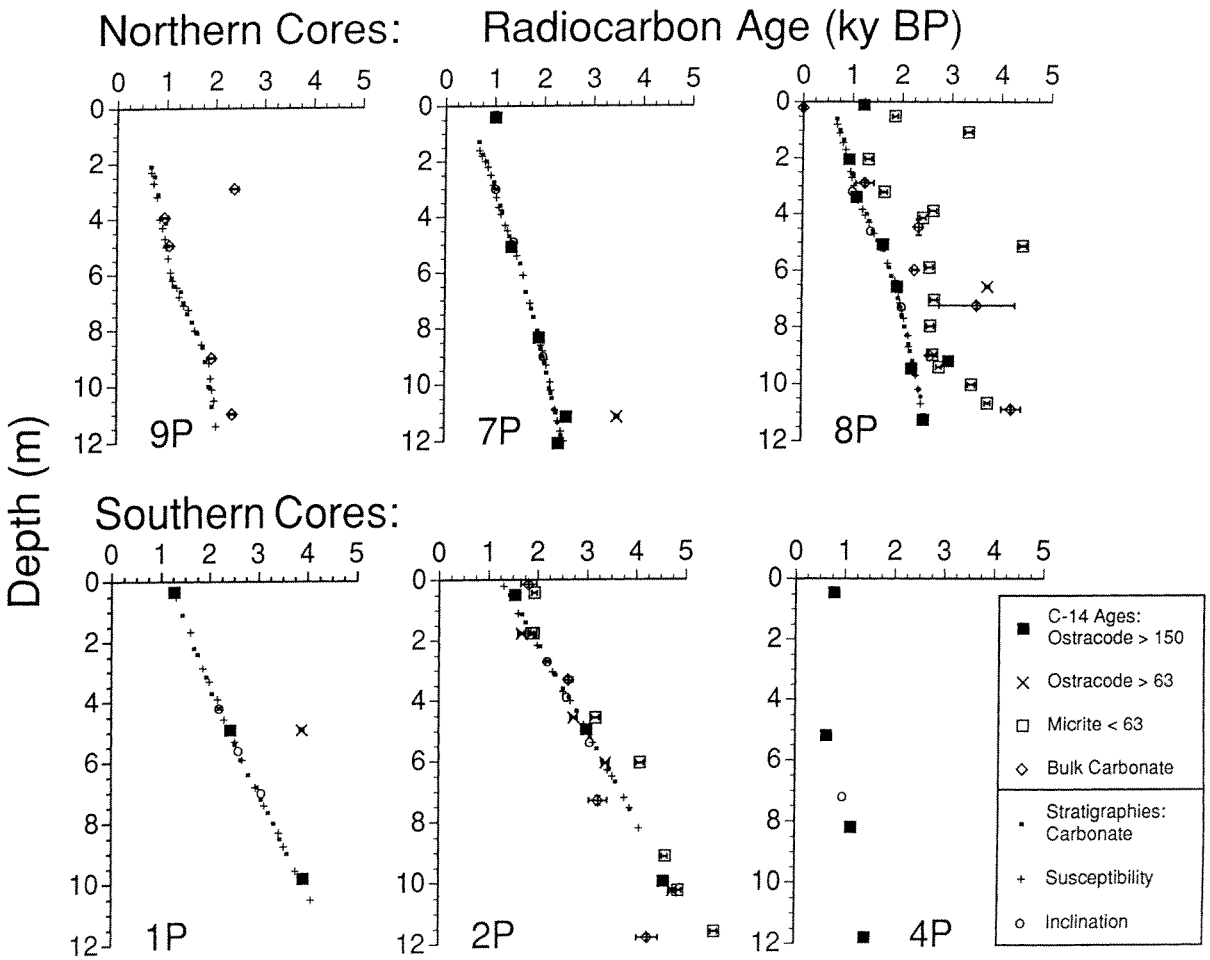

Fig. 2. ^{14}C age of various carbonate fractions versus depth down cores 1P, 2P, 4P, 7P, 8P and 9P (Table 1). Ages are corrected for isotopic fractionation using $\delta^{13}C$ measurements. Previously published ^{14}C ages that lacked $\delta^{13}C$ values were corrected assuming a $\delta^{13}C$ value of 0‰ (Halfman and Johnson, 1988; Halfman and Hearty, 1990; Halfman et al., 1992). The "average" ages defined by the >150 μm ostracode dates and stratigraphic correlations are also shown. More correlation points are plotted than listed in Table 2.

However, the presence of sediment laminations precludes this explanation. We suspect that the dates of the coarse ostracodes more closely reflect the true age of the sediments and that the older dates of the micrite result from an admixture of fine-grained calcite introduced to the lake by the strong diurnal winds that often create intense dust storms in the Turkana basin. Lacustrine sediments and soils, that may contain "old" carbonates, are exposed throughout the basin. The larger size, non-abraded nature and minimal fragmentation of the coarse ostracodes suggest that they are less susceptible than the micrite to eolian transport. Significant contributions of eolian silicates to the profundal sediments are also indicated by factor analysis of bulk sediment geochemistry of major and selected trace elements from cores 2P, 7P, 8P, 9P and 10P (Finney et al., submitted). Two end-member populations explain 95% of the variance, and are interpreted as Omo River and eolian sources.

The other cores generally do not exhibit such large age discrepancies among the carbonate fractions as are observed in 8P. The 8P site is immediately downwind of extensive Plio-Pleistocene carbonate-rich sediments and has the highest probability of eolian input with "old" carbonate. In the few cases where there are discrepancies, the coarse ostracodes almost always have the youngest dates, e.g., core 1P at 5 m depth, core 7P at 11.2 m depth (Fig. 2). Core 2P shows relatively consistent dates among all three carbonate fractions, indicating relatively low eolian input of detrital micrite at this core site. Assuming an equal flux of eolian carbonate to the 8P and 2P sites (1 wt% of the total sediment), 10–20% of the carbonate is "old" at the 8P site, whereas approximately 5% is "old" at the 2P site because of the higher carbonate content in the south basin (15–20% in 2P vs 5–10% in 8P). The difference between sites is probably underestimated due to the the suspected higher flux of "old" carbonates to the 8P site than the 2P site.

Plots of sediment age versus depth based on the >150 μm ostracode fraction are relatively linear, indicating fairly constant sedimentation rates over the time interval represented by the cores. Extrapolation of the age–depth curves to the core tops yield ages that range from 60 to 1200 yr B.I (Fig. 2). These old ages are attributed to ove penetration, bow-wave disturbance, or late trij ping of the piston core in the very fluid Turkar sediments (core-top sediment porosities >90% The oldest core-top ages occur in cores 1P and 2I Clear evidence of over-penetration was observe in the field at sites 1P and 2P. Thus, the weigh on the core-head were reduced significantly. Th younger core-top ages of the subsequent cor indicate that the extent over-penetration decrease in magnitude but was not completely eradicate The predicted depth of over-penetration of th core head beyond the sediment–water interface a sites 1P and 2P is consistent with estimates base on pore-water chemistry profiles of conservativ ions (Cerling, submitted). Less over-penetration estimated from pore-water profiles for the othe cores. Paleomagnetic inclination and declinatio profiles are significantly more disturbed in th upper 2 meters of cores 1P and 2P than at th other cores or deeper depths in 1P and 2P, and i consistent with greater over-penetration due t greater sediment compaction, wall drag an re-orientation of the magnetic minerals in th upper core tube at the disturbed sites (Kowalsk et al., 1991).

5. Correlations of carbonate and magnetic susceptibility profiles

The ostracode-based radiocarbon chronolog can be evaluated and enhanced by independen stratigraphic correlations. Carbonate profiles o cores recovered from the north basin reveal majo (m scale) and minor (cm scale) oscillations super imposed on a general trend of increasing carbonat with burial depth (Fig. 3). A number of oscilla tions can be visually correlated throughout th north basin of the lake. The increased resolutio of this data strengthen the earlier hypothesis o Halfman and Johnson (1988) that carbonate fluc tuations occur simultaneously throughout th north basin and reflect the variable discharge o detrital silicates from the Omo River and thei dilution of the autochthonous carbonates.

Temporal and spatial differences in sedimenta

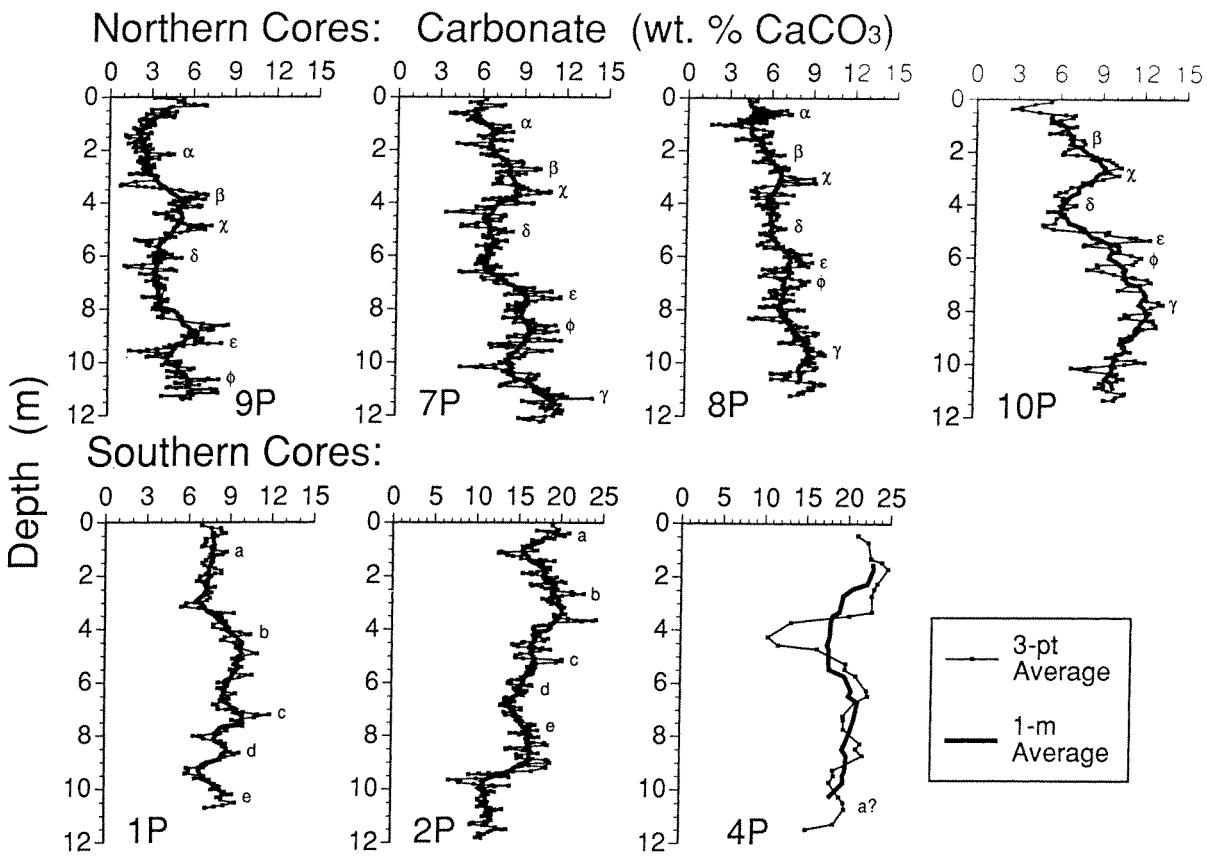

Fig. 3. Carbonate content of the dry sediment (wt% CaCO3) down cores 1P, 2P, 4P, 7P, 8P, 9P and 10P. Thin line is a 3-point running average of the data and heavy line is an 1-m running average of the data. The letters (α–γ) in the north basin and (*a–e*) in the southern basin delineate major correlation depths for the carbonate stratigraphy in the respective basins.

tion rates and core over-penetration can account for the variations among the carbonate profiles at the four north basin sites. Higher sedimentation rate at the 7P and 9P sites is consistent with closer proximity to the turbid plume from the Omo River, especially during flood season. Site 10P, situated on a slight bathymetric high and farther from the Omo Delta than the other sites in the north basin, recovered the oldest and most condensed stratigraphic section.

Will the input of "old" eolian carbonates impact the carbonate stratigraphy? Assuming a total carbonate content of 15% in 2P and 5% in 8P, and 1% of the total sediment is "old" carbonate, a linear mixing model of 9 ka carbonate with 2 ka contemporaneous carbonate yields a sample age of approximately 2.3 ka in 2P and 3.0 ka in 8P. Similar age offsets are observed between the ostracode-based chronologies and fine-grained carbonate ages in these cores. The 9 ka age is plausible because early Holocene (7–10 ka) and older carbonates (Plio-Pleistocene) are exposed in the basin, especially adjacent to the 8P site. In contrast, adding the same amount of eolian carbonate to the authigenic carbonate yields a deviation of $\pm 10\%$, which is smaller than the down-core variability, especially for the variations used in the carbonate stratigraphy. The discussion suggests that eolian carbonates may significantly alter the contemporaneous ^{14}C age of the sample but has a minor effect on the bulk carbonate content.

Magnetic susceptibility (MS) profiles reflect the

abundance of ferromagnetic material in the core, although grain size and mineralogy can influence the record (Thompson and Oldfield, 1986). The analysis of additional cores strengthens the earlier hypothesis of Halfman and Hearty (1990) that MS fluctuations reflect the input of ferromagnetic materials from fluvial (primarily the Omo), eolian, and episodic, localized volcanic sources (Fig. 4). For example, the mean MS value at the north basin sites decreases significantly with increasing distance from the Omo River. Off-scale peaks in MS, within a cm-scale interval, occur at 4.5 and 9.3 m in core 7P and 1.1 m in 2P. These peaks correspond to sub-millimeter lenses of black vo canic ash. Both core sites are just down wind fro the volcanic Central and South Islands, respe tively. Factor analysis of bulk geochemistry da for major and selected trace elements from the cores indicates that MS variations at a specific si do not correlate with the Omo or eolian en members but are most closely related to a min source of sediment to the basin that is most like of volcanic origin (Finney et al., submitted).

A number of fluctuations in the MS profiles ca be visually correlated between the four north-basi cores, with the strongest correlation between cor

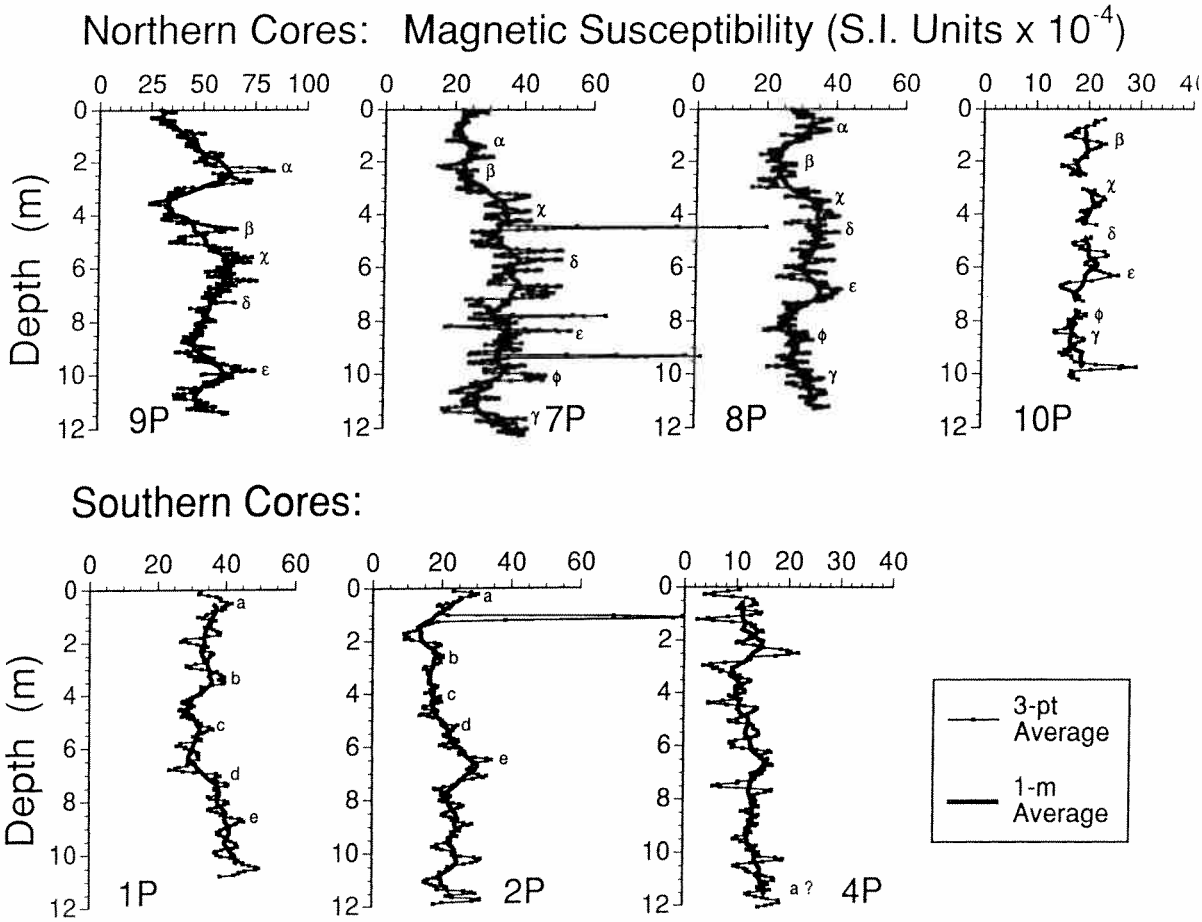

Fig. 4. Magnetic susceptibility, κ, of the archived sections of cores 1P, 2P, 4P, 7P, 8P, 9P and 10P. Thin line is a 3-point runnin average of the data and heavy line is an 1-m running average of the data. The letters (α–γ) in the north basin and (*a*–*e*) in th southern basin delineate major correlation depths for the susceptibility stratigraphy in the respective basins. The depths designate by these letters are independent of those defined in the carbonate stratigraphy (Fig. 3).

8P and 9P (Fig. 4). The spiky nature of the 7P MS profile is interpreted to reflect localized volcanic material at concentration below obvious ash layers; however, correlations can still be visualized between the smoothed profile of this core to the other sites. The down-core fluctuations in MS do not consistently co-vary with the carbonate data. For example, the relatively constant carbonate values between 5.5 and 8.5 m down 9P are incongruent with the decreasing MS values down the same interval. Yet, relatively higher values of carbonate content in 9P at 4, 9 and 11 m roughly parallel relatively lower MS values. In conclusion, MS data provides an independent stratigraphic tool to test the validity of the carbonate lithostratigraphy and ultimately the radiocarbon chronology.

The carbonate and MS profiles from two southern cores, 1P and 2P, can be correlated in a similar manner (Fig. 3 and 4). In contrast, profiles from 4P do not correlate with either 1P or 2P. The lack of correlation is consistent with the ostracode-based chronology which indicates a higher sedimentation rate, perhaps due to sediment focusing in the deep hole, and good core-top recovery at the 4P site to the extent that 4P does not significantly overlap with 1P or 2P. Stratigraphic correlations between the southern and northern cores cannot be made with the same degree of confidence as within individual basins. Isolation from the Omo River probably is the reason for the sedimentological uniqueness of the southern part of the lake (Halfman and Hearty, 1990).

Ages were assigned to each lithostratigraphic correlation point in each core, that are defined by 3-point peaks or valleys in the carbonate and magnetic susceptibility profiles, based on a linear interpolation between successive ^{14}C dates in the same core. Radiocarbon dates from $>150\ \mu m$ ostracode samples were used in cores 1P, 2P, 4P, 7P, and 8P, and from bulk carbonate samples in 9P (Table 1, 2, Fig. 2 and 5). "Old" apparent ages were avoided, e.g., core-top ostracode samples from 4P, 7P and 8P were excluded from the respective interpolations. The range in ages for the stratigraphic events for cores 7P, 8P and 9P are from 70–440 years in the north and 5–155 years in the south with a mean of 190 and 90 years, respectively. The largest discrepancy in age occurs between 9P and the other northern cores with 9P ages typically older than those calculated for 7P and 8P. It indicates that the authigenic carbonate ages from 9P are too old, especially at the bottom of the core. The interpretation is consistent with our eolian input of "old" fine-grained carbonate. Excluding 9P from the northern core averages, the range in ages for the events is reduced from 5 to 130 years with a mean of 60 years. These ranges are indistinguishable from 2σ uncertainties in the AMS ages.

Secular variability in the direction of the magnetic field provides another test for the radiocarbon chronology. Profiles from cores 1P, 2P, 4P, 7P and 8P reveal positive inflections in inclination at approximately 1, 2, 3 ka, with the oldest peak extending over the longest section of core (Kowalski et al., 1991). Lake Barombi Mbo, Cameroon, is the only site in Africa with published profiles of secular variability that span the past 5000 years. This record also reveals three peaks in inclination at approximately 1, 2 and 3 ka with the oldest peak extending over the longest section of record (Thouveny and Williamson, 1988).

For this paper, we selected the "average" ^{14}C age (calculated above) for each stratigraphic correlation point based on 7P and 8P in the northern cores and 1P and 2P in the southern cores to define the age-depth relationship. For the time-series calculations below, ages were then assigned down each core using a 5th-degree polynomial fit between the stratigraphic depths in the respective core and the "average" age. For comparison, mean sedimentation rates determined by linear, least-squares fits of the "average" age—stratigraphic depth relationships are 3.6 (1P), 2.9 (2P), 8.3 (4P), 6.2 (7P), 5.4 (8P), 6.1 (9P) and 4.8 (10P) mm/yr. Corresponding mass accumulation and carbonate accumulation rates are in Table 2. These rates are similar to estimates at other sites using ^{210}Pb, paleomagnetic, and basin-wide average sedimentation based on mass balance arguments (Yuretich, 1979; Ferguson and Harbott, 1982; Yuretich and Cerling, 1983; Barton and Torgenson, 1986; Cerling, 1986). Differences between sites can be attributed to distance from sediment sources and sediment focusing.

Table 1
New radiocarbon ages

Core depth (cm)	^{14}C Age[a] (yr B.P., $\delta^{13}C$)	$\delta^{13}C$[b] (‰, PDB)	Material	Lab. number
LT84-1P				
28–38	1260±40	−1.1	Ostracode >150 μm	AA 8664
486–496	2420±40	−0.4	Ostracode >150 μm	AA 8665
486–496	3895±45	−3.9	Ostracode 63–150 μm	AA 8666
976–986	3910±45	−1.9	Ostracode >150 μm	AA 8667
LT84-2P				
44–54	1530±40	−0.6	Ostracode >150 μm	AA 8668
490–500	2990±45	−0.9	Ostracode >150 μm	AA 8669
990–1000	4570±45	−1.9	Ostracode >150 μm	AA 8670
LT84-4P				
40–50	780±40	−2.3	Ostracode >150 μm	AA 8671
514–524	630±50	−0.1	Ostracode >150 μm	AA 9966
814–824	1130±50	−3.6	Ostracode >150 μm	AA 9967
1174–1184	1430±40	−4.4	Ostracode >150 μm	AA 8672
LT84-7P				
20–60	1005±50	1.3	Ostracode >150 μm	AA 9968
500–518	1335±50	−1.1	Ostracode >150 μm	AA 9969
828–838	1910±50	−3.5	Ostracode >150 μm	AA 9970
1109–1119	2470±40	−1.7	Ostracode >150 μm	AA 8673
1109–1119	3505±40	−0.6	Ostracode 63–150 μm	AA 8674
1202–1212	2310±40	−1.4	Ostracode >150 μm	AA 8675
LT84-8P				
0–20	1220±50	−0.5	Ostracode >150 μm	AA 9971
50–53	1850±55		<63 μm carbonate	Beta 40730, ETH 7177
106–109	3325±70		<63 μm carbonate	Beta 36355, ETH 6392
203–206	1320±65		<63 μm carbonate	Beta 36356, ETH 6393
200–210	935±50	−0.3	Ostracode >150 μm	AA 9972
321–324	1645±65		<63 μm carbonate	Beta 36357, ETH 6464
335–345	1085±100	−1.2	Ostracode >150 μm	AA 8676
388–391	2625±70		<63 μm carbonate	Beta 36358, ETH 6465
412–415	2420±60		<63 μm carbonate	Beta 40731, ETH 7178
500–515	1620±50	−0.7	Ostracode >150 μm	AA 9973
513–516	4440±75		<63 μm carbonate	Beta 36359, ETH 6466
588–591	2565±70		<63 μm carbonate	Beta 36360, ETH 6467
598–599	2265±57	0.1	Bulk carbonate	Arizona
653–663	1910±40	−1.2	Ostracode >150 μm	AA 8677
653–663	3730±45	−3.3	Ostracode 63–150 μm	AA 8678
704–707	2660±70		<63 μm carbonate	Beta 36361, ETH 6468
796–799	2590±70		<63 μm carbonate	Beta 36362, ETH 6469
896–899	2640±70		<63 μm carbonate	Beta 36363, ETH 6470
901–902	2590±60	−0.3	Bulk carbonate	Arizona
914–924	2960±40	−0.7	Ostracode >150 μm	AA 8679
940–943	2770±55		<63 μm carbonate	Beta 40732, ETH 7179
942–952	2225±40	−0.8	Ostracode >150 μm	AA 8680
1002–1005	3430±70		<63 μm carbonate	Beta 36364, ETH 6471
1067–1070	3750±55		<63 μm carbonate	Beta 40733, ETH 7180
1120–1130	2460±50	−0.7	Ostracode >150 μm	AA 9974

Table 1 (*continued*)

Core depth (cm)	^{14}C Age[a] (yr B.P., $\delta^{13}C$)	$\delta^{13}C$[b] (‰, PDB)	Material	Lab. number
LT84-9P				
291–294	2385±80		Bulk carbonate	Beta 38730, ETH 6895
393–397	960±70		Bulk carbonate	Beta 38731, ETH 6896
493–497	1060±60		Bulk carbonate	Beta 37108, ETH 6580
896–900	1940±65		Bulk carbonate	Beta 37109, ETH 6581
1096–1100	2360±60		Bulk carbonate	Beta 38732, ETH 6897

[a]Reported ages are adjusted for total isotopic effects using measured $\delta^{13}C$ values. Quoted Errors are ±1 σ based on the detection statistics.d

[b]$\delta^{13}C$ values were measured but not reported by Beta Analytic, Inc.

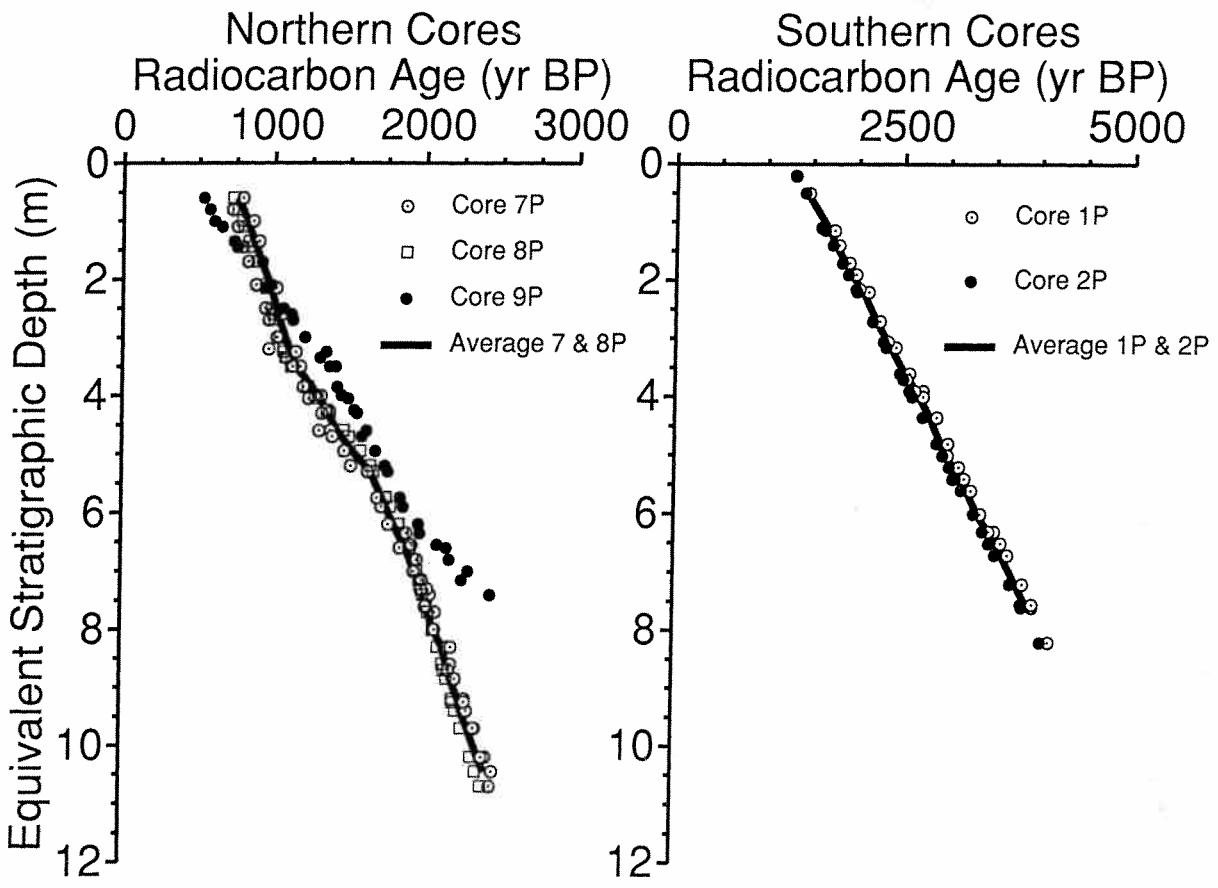

Fig. 5. ^{14}C age versus depth for the northern and southern cores. The chronology is defined by ostracode samples in cores 1P, 2P, 7P and 8P, and by authigenic carbonate samples in 9P. The depths are stratigraphically equivalent to the depth down 8P in the north and 2P in the south. More correlation points are plotted than listed in Table 2. See text for details.

Table 2
Estimated ^{14}C ages for selected stratigraphic correlations

Event[a]	Depth (cm)			Radiocarbon age[b] (yr B.P.)			Average	
	7P	8P	9P	7P	8P	9P	All	7P and 8P
Northern cores								
C-α	130	60	210	790	725	530	685	760
C-β	275	215	415	1015	945	950	970	980
C-χ	360	325	610	1145	1070	1350	1190	1110
C-δ	510	460	740	1380	1470	1615	1490	1425
C-ε	760	620	910	1765	1840	1965	1855	1800
C-ϕ	870	770	1070	1935	1955	2295	2060	1945
C-γ	1135	970		2345	2255			2300
MS-α	160	80	230	720	755	570	685	740
MS-β	250	210	430	880	940	980	935	910
MS-χ	390	350	620	1130	1115	1370	1205	1120
MS-δ	540	470	725	1390	1500	1586	1495	1445
MS-ε	860	680	1010	1955	1935	2170	2020	1945
MS-ϕ	1020	870		2170	2140			2155
MS-γ	1165	1020		2395	2320			2355
	1P	2P		1P	2P			
Southern cores								
C-a	110	50		1455	1410		1430	
C-b	420	270		2240	2160		2200	
C-c	720	520		3115	3010		3060	
C-d	850	630		3510	3385		3445	
C-e	990	760		3935	3825		3880	
MS-a	50	20		1305	1310		3060	
MS-b	330	215		2010	1970		1990	
MS-c	455	305		2330	2275		2305	
MS-d	680	480		2995	2875		2935	
MS-e	830	630		3450	3385		3415	

Sedimentation rates[c]

Core	1P	2P	4P	7P	8P	9P	10P
Sedimentation rate (mm/yr)	3.6	2.9	8.3	6.2	5.4	6.1	4.8
Average porosity[d]	0.89	0.92	0.92	0.91	0.92	0.89	0.92
Average weight% $CaCO_3$	8.3	15.7	19.7	7.97	6.6	4.2	8.9
Mass accumulation rate (mg sediment cm^{-2} yr^{-1})	100	60	175	145	110	175	100
$CaCO_3$ accumulation rate (mg $CaCO_3$ cm^{-2} yr^{-1})	8.4	9.4	34	12	7.4	7.3	8.9

[a]C is for carbonate correlations, MS is for magnetic susceptibility correlations and lower-case letters refer to correlation points i Fig. 3 and 4.
[b]Ages are rounded to nearest 5 yr.
[c]Assumes a sediment density of 2.6 g/cm^3.
[d]Data from Halfman (1987).

Lake Turkana sediments are faintly laminated with alternating light/dark couplets. Halfman and Johnson (1988) hypothesized that the couplets respond to alternating dry and wet years on an interannual (approximately 4 year) basis, perhap related to the El Niño/Southern Oscillation. Th new ostracode-based chronology significantl increases the mean sedimentation rate for 8P fron

2.7 to 5.4 mm/yr and subsequently implies that the recurrence interval for the laminae decreases from just under 4 years/couplet (2 years/lamination) to 1.0 year/lamination. The only other continuous sections of laminated sediments that are distinct enough to measure from the available cores are the upper 3 m and lower 3 m of 9P (Halfman and Hearty, 1990). The mean recurrence intervals for the upper and lower sections of 9P are 1.4 and 0.9 years/lamination, respectively, based on previous results. However, a re-examination of the laminae in the upper portion of 9P reveals very faint and previously uncounted laminae, that when counted, result in a recurrence interval of just over 0.8 years/lamination. Thus, the new AMS chronology indicates that each lamina (*not* light/dark couplet) represents an annual event. The laminations are not "varves". Perhaps each lamina is related to the seasonal flooding of the Omo River with an occasional extra event at the 9P site every few years. The exact scenario controlling the deposition of the laminae requires additional field and laboratory analyses.

6. Paleoclimatic significance

Halfman and Johnson (1988) hypothesized that the carbonate record is a record of Omo River discharge, with high carbonate values corresponding to low lake levels and low discharge of the Omo River. For example, lower lake levels imply lower Omo discharge resulting in reduced dilution of the carbonates with detrital silicates. However, this was not supported by subsequent stable isotope analyses which showed a lack of correlation between the carbonate content and $\delta^{18}O$ in core 8P (Johnson et al., 1991). A correlation was expected assuming the $\delta^{18}O$ of the carbonate fraction reflects the relative ratio of precipitation to evaporation.

Several factors may complicate the relationship between isotopic composition of the carbonate and lake level. The isotopic signal at any specific core site may be a mixture of two offsetting functions; evaporative fractionation of the lake water and distance to the Omo River delta. The extent of mixing between the isotopically light river water and isotopically heavy lake water is a function of distance from the Omo Delta; and is undoubtedly important in the north basin because the Omo River plume routinely extends past Central Island during the flood season. A 20 m drop in lake level results in a $\approx$20 km southward migration of the Omo Delta due to low topographic relief in the Omo basin. Thus a core site like 7P would be affected by more evaporated lake water causing heavier $\delta^{18}O$ values on the one hand and by closer proximity to the river mouth causing lighter $\delta^{18}O$ values on the other as well as long-term changes in the average $\delta^{18}O$ of the lake.

The bulk geochemistry data indicates that two prominent sediment populations, interpreted as Omo River and eolian sources, account for most of the variability in the profundal sediments (Finney et al., submitted). The abundance of the Omo River fraction is inversely correlated to carbonate content in the cores suggesting the dilution effect proposed by Halfman and Johnson (1988) is correct. However, the same factors outlined above may complicate a carbonate abundance and lake level relationship. Omo River discharge data are not available for a direct test. A comparison of the carbonate proxy to other high resolution climatic proxies is an alternate test of its significance.

A stacked record of carbonate abundance was constructed from cores 7P, 8P and 9P to increase the signal and decrease the noise in the individual records (Fig. 6). Data from 10P was excluded from the stack because it lacked the resolution of the other cores. To construct the stack, carbonate values in each core were normalized to units of standard deviation by subtracting the mean value from each data point and dividing the result by the standard deviation. Depths were converted to radiocarbon ages based on the polynomial fit described above. Then, a carbonate value was interpolated every 5 years down the record (approximately 3 cm) with a clamped, cubic-spline routine.

Focusing on short-term variability, the stack defines relatively lower carbonate intervals (higher Omo discharge) at two time intervals, from 0.4 to 0.8, and 1.1 to 1.7 ka (Fig. 6). A number of brief excursions to relatively lower carbonate values (higher discharge) are suggested in the older sedi-

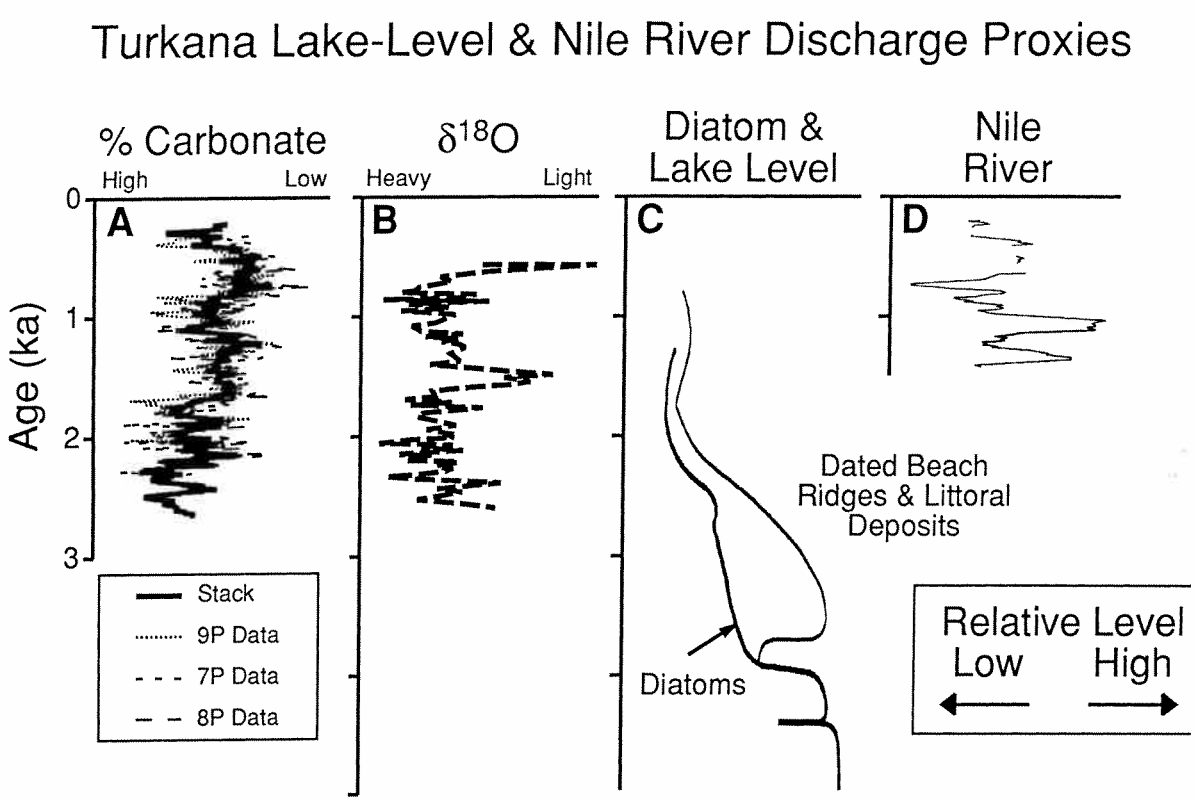

Fig. 6. Proxies of hydrologic change from Lake Turkana and the Nile River. They are plotted with increasing discharge or la level towards the right. (A) A stacked record (thick line) of carbonate abundance for the north basin of Lake Turkana. The dash lines represent individual profiles from cores 7P, 8P and 9P. (B) $\delta^{18}O$ of the fine-grained carbonate vs. age in 8P (redrawn fro Johnson et al., 1991, using the ostracode-based chronology). (C) Lake-level curves inferred from exposed beach deposits in t Turkana Basin (Owen et al., 1982) and diatom abundances in 2P (Halfman et al., 1992). (D) Nile River discharge data (redrav from Hassan, 1981, using radiocarbon instead of calendar ages).

ments at approximately 1.9, 2.1, and 2.3 ka. These inferred relative changes in the hydrologic budget are similar to other proxies from Lake Turkana. For example, peaks in $\delta^{18}O$ in 8P at 1.5 and 0.5 ka and a slight rise in lake level inferred from diatom assemblages in 2P and exposed beach deposits culminating at 1.3 ka roughly coincide with peaks in the carbonate proxy. The differences are interpreted to reflect the response times of the individual proxies, especially to migrations of the Omo Delta.

The height of the Nile Flood has been sporadically recorded since 3100 BC and almost continuously since 622 AD (Hassan, 1981). The interpretation of the record is complicated by unknown sedimentation rates in the river and changing units of measure but flood levels a generally interpreted as a barometer of hydrolog change in the Blue Nile, which drains the Ethiopia Plateau just to the west of the headwaters of th Omo River. After converting calendar years t radiocarbon years B.P. (CALIB 3.0 program, Stuiv and Reimer, 1993), relatively lower Nile discharg occurred from about 1.0 to 0.7 ka, and younge than 3.0 ka, whereas, higher flood levels occurre from about 1.3 to 1.0 ka and possibly 0.7 to 0 ka. These trends are generally similar to the ca bonate record, with the Turkana shifts precedin those observed in the Nile River proxy. A perfe correlation is not expected due to uncertainties i the ^{14}C ages, conversion between calendar an radiocarbon ages and complexities in interpretin

the records. Other climatic proxies from east Africa lack the temporal resolution for a detailed comparison.

7. Cyclic variability

Time-series analysis of individual and stacked carbonate records reveal a number of spectral peaks that are significant above the 90% confidence level and recur in most of the records (Fig. 7). These correspond to periods of about 32, 22, 18, 16 and 11 years. Precision of the AMS ages and variability introduced into the chronology by calculating the "averaged" ages may change these reported periods by about 10%. All of these peaks rise above a baseline pattern of some variance at all frequencies with a significant portion of the variance at the low frequencies. The results further support previous claims by Halfman and Johnson (1988), Halfman and Hearty (1990) and Johnson et al. (1991) of cyclic variability in climate over the Ethiopian Plateau. Our higher resolution data, new radiocarbon dates and stratigraphic correlations shorten the cycles considerably from the previously published results.

New periods at 11, 16, 18.6 and 22 years may indicate forcing mechanisms in the intensity of the northern hemisphere monsoon. For example, an 18.4-yr periodicity is observed in the discharge of the Nile River (Hameed, 1984) and an 18.5-yr periodicity in the Indian monsoon (Campbell et al., 1983). A re-examination of the lamination data utilizing the new chronology reveals periods of 11, 18.6 and 23 years that are within the resolution of the periods observed in the carbonate stack. Periods larger than 30 years have been detected in other African proxies, i.e., 31-yr in Senegal River discharge data (Faure and Gac, 1981) and 77-yr in Nile River flood data (Hameed, 1984). In addition, 80-yr cyclic variability is detected in selected El Niño/Southern Oscillation proxies (Anderson et al., 1990). Throughout the globe, high-resolution records of climate have revealed periods near 11, 18.6 and 22-yr as well, that are commonly attributed to an 18.6-yr lunar nodal, 11-yr sunspot, and 22-yr double sunspot cycles (e.g., Crowley, 1983; Morner and Karlen, 1984; Currie and Fairbridge, 1985). Finally, time-series analysis of variations in the Earth's orbit around the Sun over the past 6 ka reveals decadal periods of 11.9, 15.8, 18.6 and 29 yr as well as other shorter and longer periods (Loutre et al., 1992).

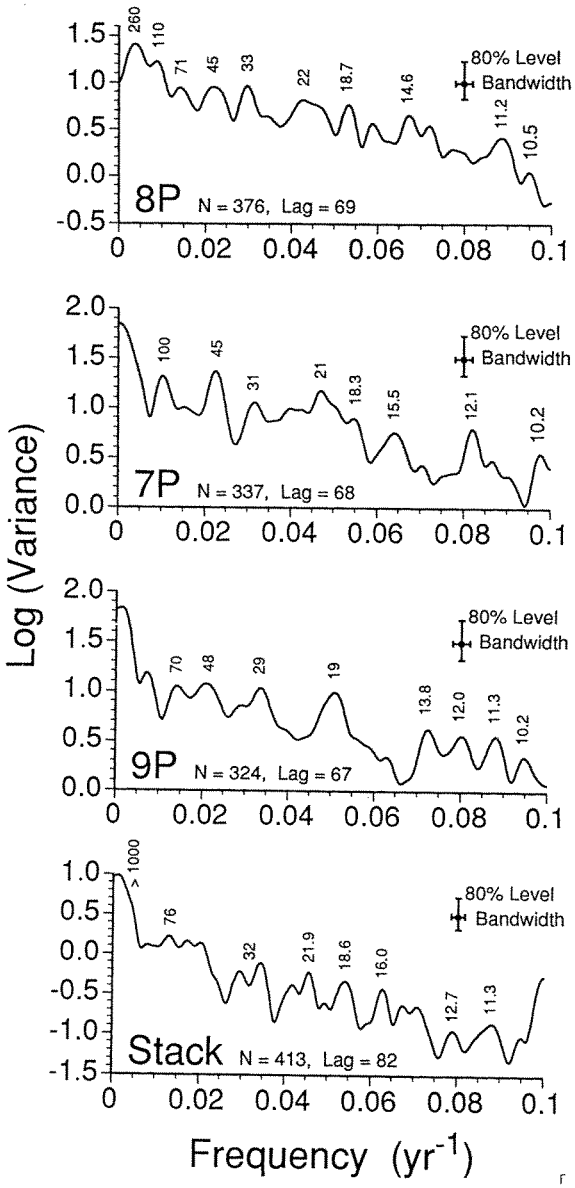

Fig. 7. Variance spectra for the individual and stacked north-basin carbonate records. Peaks in the spectra are identified by their corresponding periods (^{14}C yr/cycle).

Unfortunately, the correlation of climatic forc-

ing to decade and century scale astronomical cycles is missing a direct cause-and-effect link (Pittock, 1983), and these cycles may represent harmonics of lower frequency variability (Stuiver and Braziunus, 1989). Nevertheless, we conclude that the evidence for decadal cycles in the sedimentary record of Lake Turkana is compelling. The temporal associations between these periods and astronomical perturbations and lower frequency variability provide an intriguing subject for future study.

8. Conclusions

AMS radiocarbon dates of ostracode carapaces from piston cores recovered from Lake Turkana define a chronostratigraphy that is consistent with independent correlations of carbonate and magnetic susceptibility profiles. This chronology refines earlier estimates of sediment age in these cores that were based on a limited number of bulk carbonate samples analyzed by conventional ^{14}C methods. Variations in ^{14}C ages between different carbonate fractions suggest that eolian input of non-contemporaneous carbonate effect the radiocarbon age in this arid and windy setting. However, these inputs may have a relatively minor effect on bulk carbonate contents of the sediment. The new chronology refines the recurrence interval for each lamination from one lamination every two years to one lamination per year in two north basin cores. Stacking the north-basin carbonate profiles into a master curve provides a high-resolution proxy for hydrologic change that agrees reasonably well with other proxies from Lake Turkana but the interpretation may be complicated by migration of the Omo Delta with changing lake level. Time-series analysis of the carbonate stack reveals periods of 11, 16, 18.6, 22 and 32 yr that provide an intriguing link to other high-resolution records of climatic change.

Acknowledgements

Detailed analysis of the sediment cores was funded by NSF grants ATM 89-03649 and ATM 91-05842 awarded to JDH, ATM 91-04730 TCJ and ATM 91-06558 to BPF. We thank th Kenyan Government and Dr. E. Odada for the support in our continued research efforts at Lak Turkana. M. Wenrich provided valuable technic support for numerous analyses. N. Pisias and T Hagelberg, Oregon State University, provide valuable software and insight into Fouri Analysis. We are grateful to K. Kelts and T Cerling for their constructive comments on a earlier draft of the manuscript.

References

Anderson, R.Y., Linsley, B.K. and Gardner, J.V., 199 Expression of seasonal and ENSO forcing in climat variability at lower than ENSO frequencies: evidence fro Pleistocene marine varves off California. Palaeogeogr Palaeoclimatol., Palaeoecol., 78: 287–300.

Barton, C.E. and Torgenson, T., 1988. Palaeomagnetic an ^{210}Pb estimates of sedimentation in Lake Turkana, Ea Africa. Palaeogeogr., Palaeoclimatol., Palaeoecol., 68: 53–6

Butzer, K.W., 1971. Recent History of an Ethiopian Delt Univ. Chicago Press, 184 pp.

Campbell, W.H., Blechman, J.B. and Bryson, R.A., 198 Long-period tidal forcing of Indian monsoon rainfall: hypothesis. J. Climatol. Appl. Meteorol., 22: 289–296.

Cerling, T.E., 1986. A mass-balance approach to basi sedimentation: Constraints on the recent history of th Turkana Basin. Palaeogeogr., Palaeoclimatol., Palaeoecol 43: 129–151.

Cerling, T.E., submitted. Pore water chemistry of an alkalin lake: Lake Turkana, Kenya. In: T.C. Johnson and E. Odad (Editors), The Limnology, Climatology an Paleoclimatology of the East African Lakes.

Cerling, T.E., Bowman, J.R. and O'Neil, J.R., 1988. A isotopic study of a fluvial-lacustrine sequence: The Plic Pleistocene Koobi Fora sequence, East Africa. Palaeogeogr Palaeoclimatol., Palaeoecol., 63: 335–356.

Cohen, A.S., 1984. Effects of zoobenthic standing crop o laminae preservation in tropical lake sediments, Lak Turkana, East Africa. J. Paleontol., 58: 499–510.

Crowley, T.J., 1983. The geologic record of climatic change Rev. Geophys. Space Phys., 21: 828–877.

Currie, R.G. and Fairbridge, R.W., 1985. Periodic 18.6-yea and cyclic 11-year induced drought and flood in northwester China and some global implications. Quat. Sci. Rev. 4: 109–134.

Faure, H. and Gac, J.Y., 1981. Will the Sahelian drought enc in 1985? Nature, 291: 475–478.

Ferguson, A.D.J. and Harbott, B.J., 1982. Geographical physical and chemical aspects of Lake Turkana. In A.J. Hopson (Editor), Lake Turkana: A Report on th

Findings of the Lake Turkana Project, 1972–1975. Overseas Devel. Adm., pp. 1–107.

Finney, B.P., Halfman, J.D. and T.C. Johnson, submitted. Sediment sources in an arid rift-valley lake (Lake Turkana, Kenya)—paleoclimatic implications. Quat. Res.

Halfman, J.D., 1987. High-resolution sedimentology and paleoclimatology of Lake Turkana, Kenya. Thesis. Duke Univ., Durham, NC.

Halfman, J.D. and Johnson, T.C., 1988. High-resolution record of cyclic climatic change during the past 4 ka from Lake Turkana, Kenya. Geology, 16: 496–500.

Halfman, J.D., Johnson, T.C., Showers, W.J. and Lister, G.S., 1989. Authigenic low-Mg calcite in Lake Turkana, Kenya. J. Afr. Earth Sci., 8: 533–540.

Halfman, J.D. and Hearty, P.J., 1990. Cyclical sedimentation in Lake Turkana, Kenya. In: B. Katz (Editor), Lacustrine Basin Exploration: Case Studies and Modern Analogs. Am. Assoc. Pet. Geol. Mem., 50: 187–195.

Halfman, J.D., Jacobson, D.F., Cannella, C.M., Haberyan, K.A. and Finney, B.P., 1992. Fossil Diatoms and the mid to late Holocene paleolimnology of Lake Turkana, Kenya: a reconnaissance study. J. Paleolimnol., 7: 23–35.

Hameed, S., 1984. Fourier analysis of Nile flood level. Geophys. Res. Lett., 11: 843–845.

Hassan, F., 1981. Historic Nile floods and their implications for climate change. Science, 212: 1142–1145.

Johnson, T.C., Halfman, J.D., Rosendahl, B.R. and Lister, G.S., 1987. Climatic and tectonic effects on sedimentation in a rift-valley lake: Evidence from Lake Turkana, Kenya. Geol. Soc. Am. Bull., 98: 439–447.

Johnson, T.C., Halfman, J.D. and Showers, W.J., 1991. Paleoclimate of the past 4000 years at Lake Turkana, Kenya based on isotopic composition of authigenic calcite. Palaeogeogr., Palaeoclimatol., Palaeoecol., 85: 189–198.

Jones, G.A. and Kaiteris, P., 1983. A vacuum-gasometric technique for rapid and precise analysis of calcium carbonate in sediments and soils. J. Sediment. Petrol., 53: 655–660.

Kowalski, E.A., Halfman, J.D. and King, J.W., 1991. New geochronologic controls on paleoclimatic signals from Lake Turkana, Kenya. EOS Trans. Am. Geophys. Union Abstr. with Program, 72: 271–272.

Kutzbach, J.E. and Street-Perrott, F.A., 1985. Milankovitch forcing of fluctuations in the level of tropical lakes from 18 to 0 kyr BP. Nature, 317: 130–134.

Loutre, M.F., Berger, A., Bretagnon, P. and Blanc, P.L., 1992. Astronomical frequencies for climate research at the decadal to century time scale. Clim. Dyn., 7: 181–194.

Morner, N.A. and Karlen, W. (Editors), 1984. Climatic Changes on a Yearly to Millennial Basis. Reidel, Dordrecht, 667 pp.

Owen, R.B., Barthelme, J.W., Renant, R.W. and Vincens, A., 1982. Palaeolimnology and archaeology of Holocene deposits north-east of Lake Turkana, Kenya. Nature, 298: 523–528.

Pittock, A.B., 1983. Solar variability, weather and climate: an update. Q. J. R. Meteorol. Soc., 109: 23–55.

Street-Perrott, F.A. and Harrison, S.P., 1983. Lake levels and climate reconstructions. In: A.D. Hecht (Editor), Paleoclimate Data and Modeling. Wiley, New York, pp. 291–304.

Stuiver, M. and Braziunus, T.F., 1989. Atmospheric ^{14}C and century-scale solar oscillations. Nature, 338: 405–408.

Stuiver, M. and Reimer, P.J., 1993. Extended ^{14}C data base and revised CALIB 3.0 ^{14}C age calibrations program. Radiocarbon, 35: 215–230.

Thompson, R. and Oldfield, F., 1986. Environmental Magnetism. Allen and Unwin, 227 pp.

Thouveny, N. and Williamson, D., 1988. Palaeomagnetic study of the Holocene and Upper Pleistocene sediments from Lake Barombi Mbo, Cameroon: first results. Phys. Earth Planet. Inter., 52: 193–206.

Yuretich, R.F., 1979. Modern sediments and sedimentary processes in Lake Rudolf (Lake Turkana) eastern rift valley, Kenya. Sedimentology, 26: 313–331.

Yuretich, R.F., 1986. Controls on the composition of modern sediments, Lake Turkana, Kenya. In: L.E. Frostick et al., (Editors), Sedimentation in the African Rifts. Geol. Soc. Spec. Publ., 25: 141–152.

Yuretich, R.F. and Cerling, T.E., 1983. Hydrogeochemistry of Lake Turkana, Kenya: Mass balance and mineral reactions in an alkaline lake. Geochim. Cosmochim. Acta, 47: 1099–1109.